A finite lattice study of the critical behaviour of the two-dimensional biaxial next-nearest-neighbour Ising model

1987 J. Phys. A: Math. Gen. 20 1507

(http://iopscience.iop.org/0305-4470/20/6/033)

J. Phys. A: Math. Gen. **20** (1987) 1507–1519. Printed in the UK

A finite lattice study of the critical behaviour of the two-dimensional biaxial next-nearest-neighbour Ising model

J Oitmaa†, Murray T Batchelor‡ and Michael N Barber‡

† School of Physics, The University of New South Wales, Kensington, NSW 2033, Australia
‡ Department of Mathematics, Faculty of Science, The Australian National University, Canberra, ACT 2601, Australia

Received 28 July 1986

Abstract. The critical behaviour of an Ising model with competing first- and third-nearest-neighbour interactions ('biaxial next-nearest-neighbour Ising' or 'BNNNI' model) on the square lattice is investigated by finite lattice methods. In the ferromagnetic region, the phase boundary is located with an accuracy at least equal to that of alternative methods. In the antiphase region, distinctive structure in finite lattice estimators is found over an extended temperature range. However, the nature of the transition remains unclear.

1. Introduction

Systems with competing interactions are now known to be capable of yielding rich and complex critical behaviour. Ising systems with competing ferromagnetic and antiferromagnetic interactions can exhibit a rich variety of ordered phases at low temperatures, including modulated phases (Selke 1984). The nature of the phase transition can also vary quite dramatically, with the occurrence, in particular cases, of non-universal behaviour, first-order transitions and multicritical points.

In this paper we report on a finite lattice study of the square lattice Ising model with first- and third-nearest-neighbour interactions, described in the preceding paper (Oitmaa and Velgakis 1987). The model is described by the Hamiltonian ($s_i = \pm 1$)

$$H = -J \sum_{\langle ij \rangle} s_i s_j - J' \sum_{[ij]} s_i s_j \tag{1}$$

where the summations run over nearest- and next-nearest-neighbour pairs in both axial directions, respectively. Without loss of generality, we restrict attention to ferromagnetic nearest-neighbour interactions ($J > 0$). In two dimensions, this model is the isotropic version of the ANNNI model discussed by Hornreich *et al* (1979) and Selke and Fisher (1980). We choose to call the model the 'biaxial next-nearest-neighbour Ising' or 'BNNNI' model.

Depending on the values of the interaction parameters, J and J', the Hamiltonian (1) has three basic types of ground state. These are the ferromagnetic (F), antiferromagnetic (AF) and 'antiphase' (AP) states, shown in figure 1(a). Three of the degenerate antiphase states are shown in figure 1(b). In each case the (2, 2) antiphase state of the ANNNI model is present along both axial directions. The 'chessboard' state has an eightfold degeneracy while the 'staircase' configurations are each fourfold degenerate.

0305-4470/87/061507+13$02.50

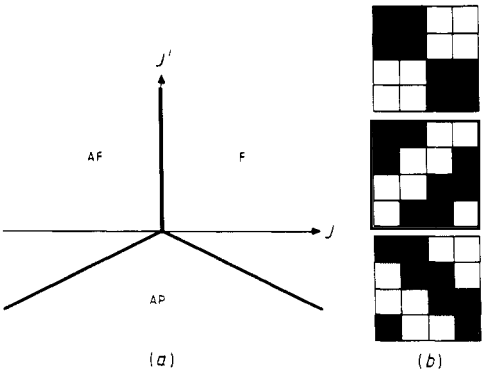

Figure 1. (*a*) Possible ground states of Hamiltonian (1) as a function of J and J': F ferromagnetic, AF antiferromagnetic, AP antiphase ordered. (*b*) Three of the possible antiphase ground states. The top figure represents a chessboard configuration while the remaining two figures are both staircase configurations. Here open and shaded squares represent up and down spins.

The transition from the ferromagnetic ground state is expected to be a universal two-dimensional Ising transition. For $J' < -J/2$ the nature of the transition, or sequence of transitions from the commensurately modulated chessboard configuration to the high-temperature disordered phase, is uncertain. Early Monte Carlo work (Hornreich *et al* 1979, Selke and Fisher 1980) indicated a transition from the commensurate phase to an incommensurate phase followed by a second transition to the disordered phase, this transition presumably being of Kosterlitz-Thouless type. However, the more recent Monte Carlo study of Landau and Binder (1985) suggests that there is no intermediate phase. Rather, the commensurate and disordered phases are separated by a single first-order transition. The series analysis of Oitmaa and Velgakis, in the preceding paper, tends to support the picture of two transitions, although the evidence is far from conclusive.

To explore the nature of the transitions from the ferromagnetic and antiphase states by a different technique and to hopefully resolve the above conflict we have applied 'phenomenological renormalisation' (Nightingale 1976). (For recent reviews see Nightingale (1982) and Barber (1983).) Our results for the ferromagnetic transition agree with those of the previous studies. Unfortunately, our results for the case with third-nearest neighbours sufficiently strongly antiferromagnetic (the transition from the chessboard ground state) are inconclusive and give no definite support for either scenario.

The paper is arranged as follows. In § 2 we write down the transfer matrix and discuss the nature of the leading eigenvalues. A detailed discussion of the transition from the ferromagnetic state is presented in § 3. In § 4 we examine the nature of the transition in the antiphase region and concluding remarks are made in § 5.

2. The method

The method of 'phenomenological renormalisation' is based on computation from the appropriate transfer matrices, of the correlation length for a sequence of $m \times \infty$ strips,

followed by a scaling analysis. This approach has proven to be highly successful for a variety of two-dimensional systems (Nightingale 1982, Barber 1983).

In the present study the most convenient choice of strips is in the diagonal direction as shown in figure 2, where the successive 'rows' have a zig-zag form. This choice has two advantages: firstly, only neighbouring rows are coupled by the interactions, and secondly, the natural modulation direction lies parallel to the strip direction.

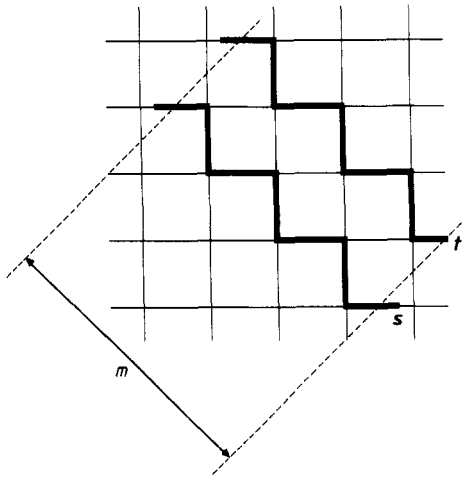

Figure 2. Diagonal rows of spins s and t on the square lattice used to define the transfer matrix $T(s, t)$ on a strip of width m.

If the spin configurations of two adjacent rows are specified by $s = (s_1, s_2, \ldots, s_m)$ and $t = (t_1, t_2, \ldots, t_m)$ then the $2^m \times 2^m$ transfer matrix $T(s, t)$ can be written as

$$T(s, t) = \varphi_0(s)\varphi_1(s, t)\varphi_2(s, t) \tag{2}$$

where

$$\varphi_0(s) = \exp\left(K \sum_{i=1}^{m} s_i s_{i+1} \right) \tag{3a}$$

$$\varphi_1(s, t) = \exp\left(K \sum_{i=1}^{m/2} s_{2i}(t_{2i-1} + t_{2i+1}) \right) \tag{3b}$$

$$\varphi_2(s, t) = \exp\left(K' \sum_{i=1}^{m} s_i(t_{i-2} + t_{i+2}) \right) \tag{3c}$$

with $K = J/kT$, $K' = J'/kT$. Periodic boundary conditions between edges of the strip are assumed implicitly in (2) and this requires that the strip width, m, is even. In addition, for $K' < -K/2$, m must be a multiple of four to incorporate the possible antiphase states.

For a specified choice of the coupling constants K, K', we have computed the leading eigenvalues of the transfer matrix by two methods. The first approach was to use translational symmetry along the rows, and spin reversal symmetry to construct a set of symmetrised states which block diagonalised the transfer matrix. It is in fact only necessary to consider two sectors, that which is invariant under both translations and

spin reversal and that which is invariant under translations but changes sign under spin reversal. The dominant eigenvalue λ_0 is contained in the first sector, while the latter sector contains the first subdominant eigenvalue λ_1. Using this approach the largest strip considered was of width $m = 12$, giving matrices of size 356×356 and 344×344. The second approach was to factor the full $2^m \times 2^m$ transfer matrix into a product of sparse matrices (Nightingale 1979, Batchelor 1986). Some details of the factorisation are given in the appendix. This technique enabled us to compute the leading eigenvalues for $m = 16$, which was necessary for investigation of the transition for $\alpha < -\frac{1}{2}$.

To find the dominant eigenvalues in each sector, we used the power algorithm as modified by Faddeev and Faddeeva (1963) to allow for the dominant eigenvalue being a complex conjugate pair.

The nature of the leading eigenvalues λ_0, λ_1, λ_2 ($\lambda_0 > |\lambda_1| \geq |\lambda_2| \ldots$) is shown schematically in figure 3 as a function of the coupling constants K, K'. We note four points.

(i) The dominant eigenvalue λ_0 is everywhere real, positive and non-degenerate.

(ii) For a given K' all eigenvalues are symmetric in K. For λ_0 this reflects the fact that the free energy is an even function of K; for λ_1 it is a consequence of the diagonal direction of the strip—the diagonal correlations are unchanged on changing the sign of K.

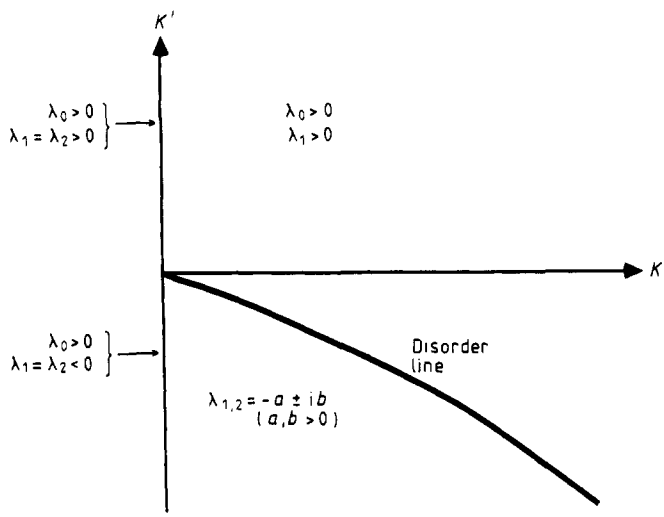

Figure 3. Schematic illustration of the nature of the leading eigenvalues of the transfer matrix as a function of K and K'.

(iii) For $K' > 0$, and for part of the region $K' < 0$, the subdominant eigenvalue λ_1 is real, positive and non-degenerate. In the remainder of the region $K' < 0$, separated from the previous part by a 'disorder line', the subdominant eigenvalue is a complex conjugate pair with negative real part.

(iv) Along the axis $K = 0$, the dominant eigenvalue is symmetric in K' and the subdominant eigenvalue is real and doubly degenerate. In this limit the model consists of four independent, interpenetrating, lattices with nearest-neighbour coupling K'.

The inverse correlation length, which describes the decay of correlations in the infinite direction of the strip, is obtained as

$$\xi_m^{-1} = \ln(\lambda_0/|\lambda_1|) \tag{4}$$

and the finite-size scaling assumption (Nightingale 1976, Barber 1983) is that, at criticality, this scales inversely with the width of the strip. Thus the equation

$$m\xi_m^{-1}(K, K') = m'\xi_m^{-1}(K, K') \tag{5}$$

gives, for a sequence of values m, m', a sequence of estimates of the critical point.

More generally, to allow for the possibility of anisotropic scaling, one considers the quantities (Domany and Kinzel 1981, Barber 1983)

$$Y_{m,m'} = \frac{\ln(\xi_m/\xi_{m'})}{\ln(m/m')} \tag{6}$$

and obtains estimates of the critical point from intersections of successive Y. In regions where the correlations are oscillatory, the scaling behaviour of the modulation wavevector can also yield useful information (Duxbury *et al* 1984). The appropriate quantity is

$$Z_{m,m'} = \frac{\ln(\delta q_{m'}/\delta q_m)}{\ln(m/m')} \tag{7}$$

with

$$\delta q_m = \frac{1}{2\pi}\tan^{-1}\left(\frac{\mathrm{Im}(\lambda_1)}{\mathrm{Re}(\lambda_1)}\right) - q_0 \tag{8}$$

and where q_0 is the characteristic wavevector of the ground state.

We now proceed to describe and discuss our results.

3. The ferromagnetic region

In the ferromagnetic region ($\alpha > -0.5$) a single Ising-like transition is expected and this is borne out by our results. In figure 4(a) we show a plot of the quantities $Y_{m,m-2}$ (6) against temperature for the case $\alpha = -0.2$. The curves clearly show the expected scaling behaviour with a common crossover point at $kT/J \approx 1.41$. Furthermore the scaling appears to be isotropic, so that the phase boundary can be determined by solving the equation

$$m\xi_m^{-1}(K, \alpha K) = (m-2)\xi_{m-2}^{-1}(K, \alpha K) \tag{9}$$

numerically, for a fixed α. The sequences of finite lattice estimates obtained in this way, for $\alpha = 0.5$, 0, -0.2, -0.4, are shown in table 1. In all cases, the estimates for $m > 8$ appear to be converging at a rate close to m^{-3} in accord with the expected convergence rate for an Ising system (Barber 1985). The extrapolated value listed in the table was obtained by fitting estimates from two successive lattice pairs to the form $a + bm^{-3}$; the error bar being a (subjective) indication of the reliability of this extrapolation.

The critical temperatures obtained in this way are in agreement with the Monte Carlo results of Landau and Binder (1985) and with the series estimates obtained in the preceding paper. However the transfer matrix method used here is able to handle

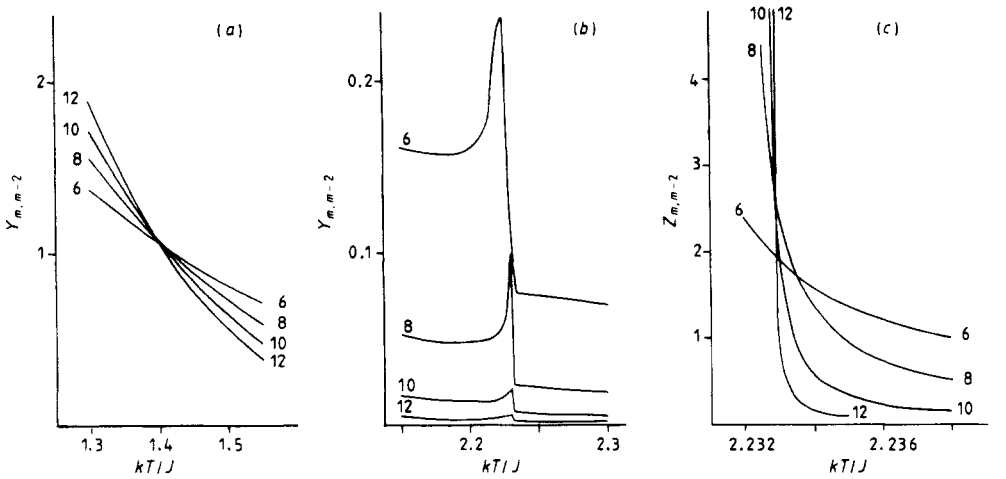

Figure 4. The scaling estimators $Y_{m,m-2}$ and $Z_{m,m-2}$ as functions of temperature for $\alpha = -0.2$ for the indicated values of m. (*a*) The correlation length estimator $Y_{m,m-2}$. Successive curves cross at the finite lattice estimates of the transition temperature. (*b*) Peaks in $Y_{m,m-2}$ at a higher temperature indicating the presence of a disorder point. (*c*) The wavevector estimator $Z_{m,m-2}$. Successive curves cross at the finite lattice estimates of the disorder temperature.

Table 1. Estimates of the critical temperature kT_c/J, obtained from finite width strips.

	α			
m/m'	0.5	0.0	−0.2	−0.4
6/4	4.060 14	2.238 33	1.424 77	0.514 66
8/6	4.059 58	2.256 96	1.420 13	0.505 14
10/8	4.093 61	2.263 19	1.416 19	0.498 52
12/10	4.103 40	2.265 83	1.413 98	0.494 67
14/12	4.109 67	2.267 12	1.412 75	0.492 37
Extrapolation	4.120 ± 0.0006	2.2691 ± 0.0002 exact = 2.269 18 . . .	1.4105 ± 0.0005	0.488 ± 0.001

the region near the multiphase point $\alpha = -0.5$, where the series method is unsuccessful. The critical line is shown in figure 5. We also show the approximate phase boundary obtained by Hornreich *et al* (1979), using the method of Müller-Hartmann and Zittartz (1977), which gives

$$kT/J = \frac{2(1+2\alpha)}{\ln(1+\sqrt{2})}. \tag{10}$$

Estimates of the correlation length exponent ν can be obtained from finite lattice estimates of the quantities

$$\omega_m = \frac{\partial}{\partial T}\xi_m^{-1} \tag{11}$$

since standard scaling arguments imply that

$$\frac{\ln(m\omega_m(T_c)/m'\omega_{m'}(T_c))}{\ln(m/m')} \to \nu^{-1} \qquad \text{as } m \to \infty. \tag{12}$$

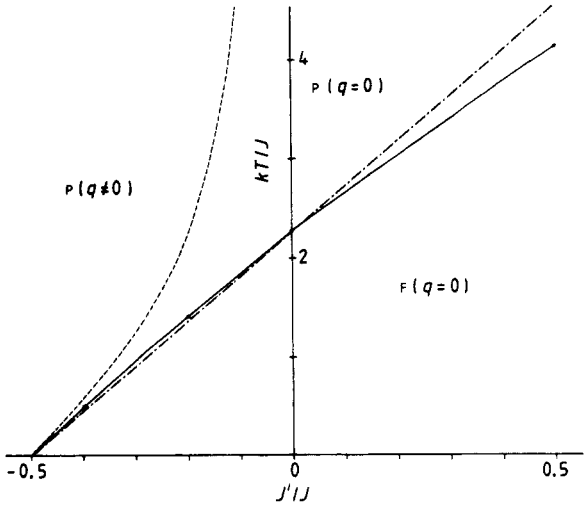

Figure 5. The ferromagnetic phase boundary of the BNNNI model. Curves: (——) transition temperatures as determined from finite width strips, (- - -) the disorder line (see text) and (—·—) the approximation (10) of Hornreich *et al* (1979).

These estimates are shown in table 2 and are clearly consistent with a limiting value of $\nu = 1$, confirming the universal nature of the transition throughout the ferromagnetic region.

Most systems with competing interactions exhibit a disorder line (Stephenson 1970), which separates regions of monotonically decaying and oscillatory correlations in the paramagnetic phase. In the present case we have used two related methods to locate the disorder line. The crossover from monotonic to oscillatory decay of correlations corresponds to the merging of the second and third largest eigenvalues of the transfer matrix into a complex conjugate pair. Thus, for a given α, the disorder point corresponds to the K value at which these eigenvalues merge. This gives a rapidly converging sequence of estimates with increasing strip width.

The location of the disorder line can also be obtained from the quantities $Y_{m,m'}$ and $Z_{m,m'}$ defined in the previous section. In this we follow the work of Beale *et al* (1985), who used this approach to locate the disorder line for the two-dimensional ANNNI model. For given α, the disorder line is expected to lead to a sharp peak in the $Y_{m,m-2}$ at the disorder temperature, and this is clearly seen in figure 4(*b*) for the

Table 2. Estimates of the critical exponent ν.

	α			
m/m'	0.5	0.0	−0.2	−0.4
6/4	0.9908	1.039	1.107	1.575
8/6	0.9952	1.021	1.048	1.229
10/8	0.9968	1.013	1.024	1.096
12/10	0.9974	1.009	1.013	1.041
14/12	0.9986	1.007	1.007	1.014

case $\alpha = -0.2$. However the height of the peak decreases rapidly for increasing strip width and it is more convenient to examine the quantities $Z_{m,m-2}$. These are shown in figure 4(c) and are seen to scale at the disorder temperature. The location of the disorder line is shown in figure 5.

To conclude this section we briefly discuss the applicability of consequences of conformal invariance to the BNNNI model along the ferromagnetic critical line. Isotropic, translationally invariant systems with short-range interactions are believed to be conformally invariant at criticality. In two dimensions, this has a number of significant implications. (For a recent review see Cardy (1986).) In particular, for a transfer matrix of a strip of finite width m, conformal invariance predicts (Cardy 1984)

$$\text{(i)} \quad \varepsilon_0 \equiv \lim_{m\to\infty} m\xi_m^{-1} = \frac{a_t}{a_x}\pi\eta \tag{13}$$

and (Blöte *et al* 1986, Affleck 1986)

$$\text{(ii)} \quad \delta_0 \equiv \lim_{m\to\infty} (\beta f_\infty - \beta f_m)m^2 = \frac{a_t}{a_x}\frac{\pi c}{6} \tag{14}$$

where

$$\beta f_m = -\ln \lambda_0 / m \tag{15}$$

is the free energy per site. In (13) and (14), a_t and a_x are respectively the units of length along and perpendicular to the strip direction and c is the conformal anomaly.

In the present case, we have $a_t = \sqrt{2}$ and $a_x = 1/\sqrt{2}$ from the orientation of the strip (recall figure 2). Hence, on assuming that the ferromagnetic transition of the BNNNI model is Ising-like, so that $c = \frac{1}{2}$ and $\eta = \frac{1}{4}$, we obtain the predictions

$$\delta_0 = \pi/6 \qquad \text{and} \qquad \varepsilon_0 = \pi/2. \tag{16}$$

Finite lattice estimates of δ_0 were obtained from successive strips using a simple two-point fit to $-\beta f_m$ as a linear function of $1/m^2$. The resulting estimates against $1/m$ are shown in figure 6(a) for $\alpha = 0.5$, 0, -0.2 and -0.4, where in each case we

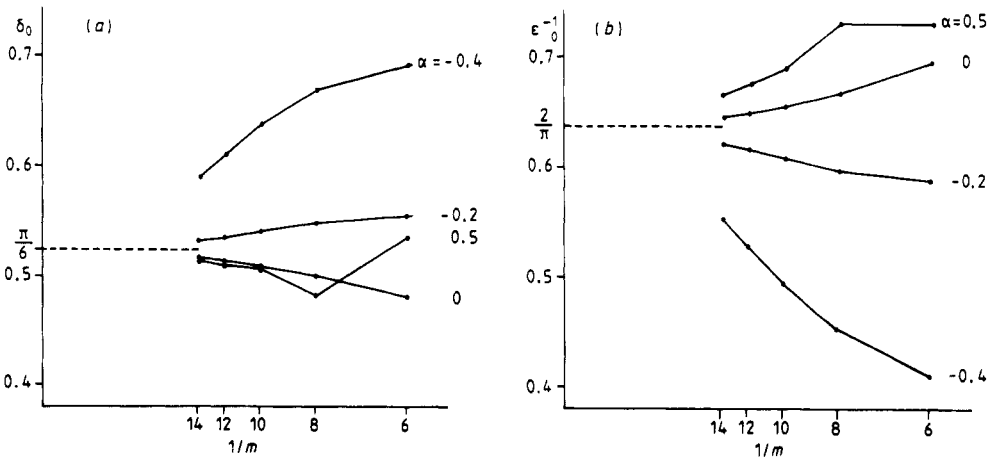

Figure 6. Plots of (a) $(\beta f_\infty - \beta f_m)m^2$ and (b) ξ_m/m against $1/m$ for $\alpha = -0.4$, -0.2, 0 and 0.5. The expected (universal) limits predicted by conformal invariance are shown by the broken line.

used the corresponding (central) estimate of the bulk critical temperature shown in table 1(a). These estimates are not particularly sensitive to variations of the temperature within the errors quoted in table 1(a). Clearly, the trend with increasing m is consistent with the expected limit for all α, although for $\alpha = -0.4$ the approach to this limit is evidently quite slow.

The corresponding trend in estimates of the quantities $m\xi_m^{-1}$ at the (estimated) bulk critical temperatures results in either over- or underestimation of the expected limit for ε_0. This reflects on over- or underestimation of the bulk critical temperature and clearly *assuming* (13) could be used as a means of sharpening our estimates of T_c. A better test of (13) is obtained if $m\xi_m^{-1}$ is computed at the $m/(m-2)$ estimate of the critical temperature. These quantities are plotted against $1/m$ in figure 6(b) and illustrate a clear trend towards the expected universal limit.

4. The antiphase region

The more interesting region of the phase diagram for the BNNNI model is the region $\alpha < -0.5$, in which the ground state is the chessboard or staircase configuration (figure 1(b)). We wish to distinguish between the two possible scenarios:

(i) two transitions with an intermediate incommensurately modulated phase (Selke and Fisher 1980);

(ii) a single first-order transition (Landau and Binder 1985).

A finite lattice method, using the quantities Y_m and Z_m (equations (6) and (7)), should in principle be able to locate and distinguish between commensurate, incommensurate and paramagnetic phases.

For the chiral clock model (Duxbury *et al* 1984) and the ANNNI model (Beale *et al* 1985) it is found that Y_m does not scale at the commensurate to incommensurate phase boundary, but the quantity Z_m does. However Y_m does scale at the higher-temperature incommensurate to paramagnetic phase boundary. Thus the presence of two transitions, separated by an incommensurate phase, is indicated by the scaling of Y_m and Z_m at two distinct temperatures.

In order to accommodate the possible antiphase states for the BNNNI model it is necessary to choose strips whose width is a multiple of four. In figures 7 and 8 we show plots of $Y_{m,m-4}$ and $Z_{m,m-4}$ as functions of temperature, for the two cases $\alpha = -0.75$ and $\alpha = -1.0$. We also show in these figures the Monte Carlo (Landau and Binder 1985) and series (Oitmaa and Velgakis 1987) estimates of the transition temperature. In both cases the Y functions show behaviour quite different from the ferromagnetic region (cf figure 4(a)). There is some indication of scaling at a temperature slightly below the Monte Carlo estimate, followed by a loop and then a rapid decrease in Y. From the $m = 8$ curve it is tempting to conclude that the Y function is developing a flat region of finite extent, indicative of an incommensurate phase with an algebraic decay of correlations. However the larger m results destroy this viewpoint and, surprisingly, the loop appears to become more pronounced for larger m. The peak in Y_m occurs near the series estimate of a transition temperature.

There is some ambiguity in the definition of the Z_m functions in the antiphase region. The chessboard ground state and one of the staircase structures clearly have a modulation wavelength of two 'rows', and hence a wavevector of $q_0 = \frac{1}{2}$. However, the other staircase structure is fully periodic in the direction of the strip and hence would have a $q_0 = 0$. Since the chessboard phase is dominant at finite temperatures,

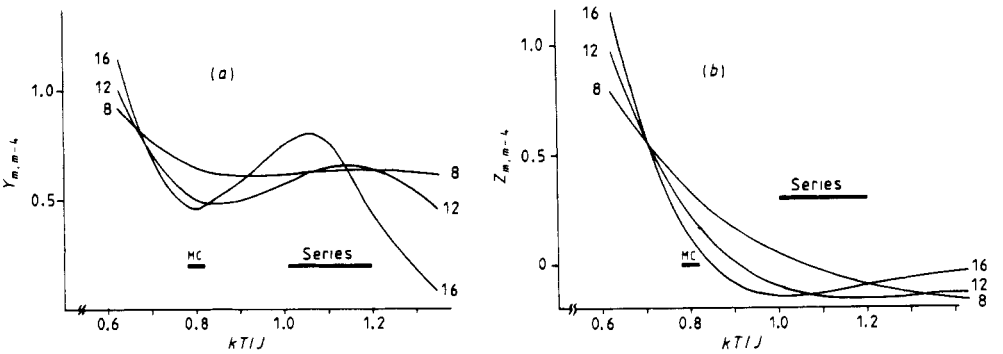

Figure 7. The scaling estimators, $Y_{m,m-4}$ and $Z_{m,m-4}$, as functions of temperature for $\alpha = -0.75$. (a) The correlation length estimator $Y_{m,m-4}$. (b) The wavevector estimator $Z_{m,m-4}$. Also shown are the corresponding Monte Carlo and series estimates of the transition temperature.

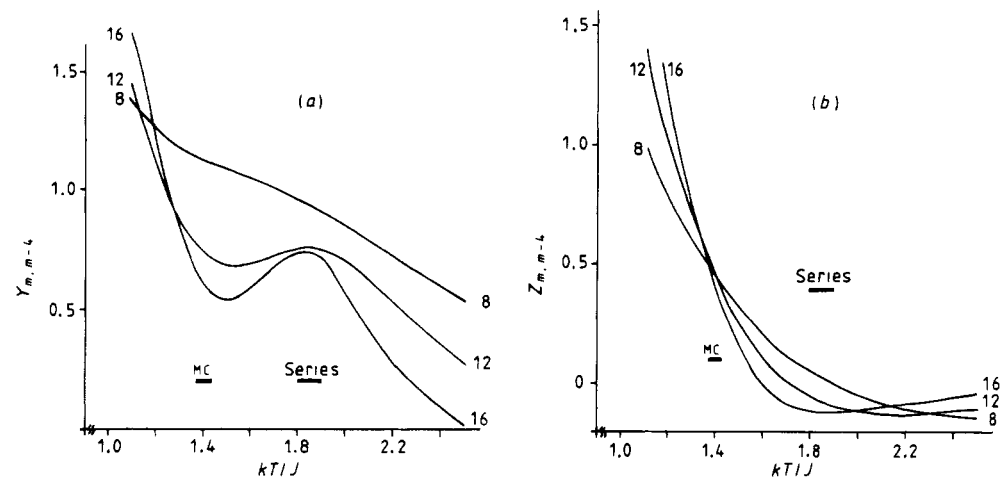

Figure 8. Scaling estimators as a function of temperature for $\alpha = -1.0$. (a) The correlation length estimator $Y_{m,m-4}$. (b) The wavevector estimator $Z_{m,m-4}$. Also shown are the corresponding Monte Carlo and series estimates.

because of higher entropy, we use $q_0 = \frac{1}{2}$ in defining the Z_m functions. For $\alpha = -0.75$ the Z_m show a consistent scaling behaviour at a temperature slightly below the Monte Carlo estimate, as shown in figure 7(b). Figure 8(b) shows Z_m for $\alpha = -1.0$, and again there is an indication of scaling behaviour near the Monte Carlo estimate. In neither case is there any indication of scaling near the series estimate.

As the antiferromagnetic interactions become stronger the behaviour of the Y_m functions becomes more like the standard Ising case. In figure 9 we show these functions for $\alpha = -2.0$. The curves for $m = 8$ and 12 suggest a single conventional (continuous) transition. However, the curve for $m = 16$ indicates the beginning of possible structures similar to that seen for larger values of α.

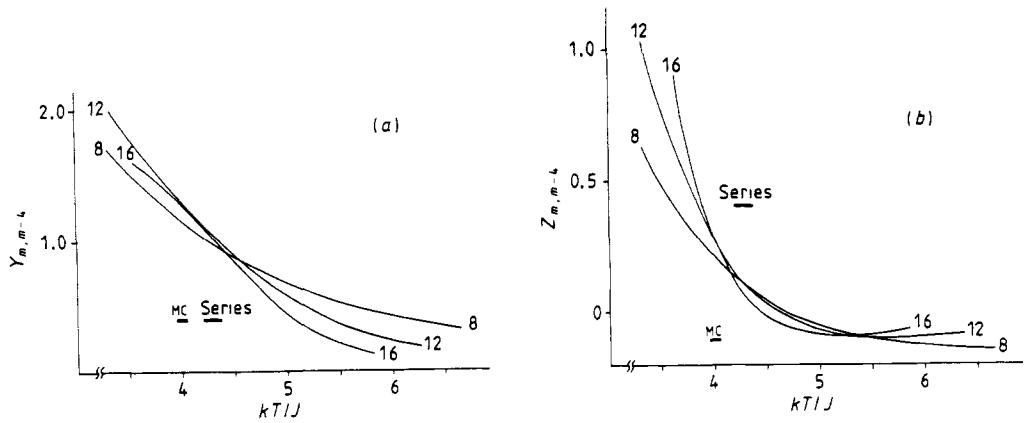

Figure 9. Scaling estimators as a function of temperature for $\alpha = -2.0$. (*a*) The correlation length estimator $Y_{m,m-4}$. (*b*) The wavevector estimator $Z_{m,m-4}$. Also shown are the corresponding Monte Carlo and series estimates.

5. Conclusions

We have carried out extensive studies of the biaxial next-nearest-neighbour Ising model using the well known technique of transfer matrix calculations for finite width strips and scaling arguments. The novel feature of our approach, namely the choice of strips in the diagonal direction with zig-zag rows, allows us to treat quite large strips with widths up to $m = 16$.

Despite the large amount of data our analysis is inconclusive, at least in the most interesting part of the phase diagram. In the ferromagnetic region, we locate the phase boundary with an accuracy at least equal to the series results of the preceding paper and obtain clear evidence that the transition is an Ising transition. However in the antiphase region we are unable to decide in favour of two successive transitions or a single first-order transition. Interestingly we do find distinctive structures in finite lattice estimators at two different temperatures, or rather over an extended temperature range. This would explain why the series and Monte Carlo results find apparent transitions at two distinct temperatures.

Clearly the true behaviour is quite subtle and a final resolution is not likely to be easy.

Acknowledgments

One of the authors (MTB) gratefully acknowledges support from a Commonwealth Postgraduate Research Award and, while at the University of New South Wales, further assistance from a Gordon Godfrey Scholarship. This work forms part of a project which is being supported by the Australian Research Grants Scheme.

Appendix. Sparse matrix factorisation of the transfer matrix

Each transfer matrix element between spin sets s and t in figure 2 can be written as a product of Boltzmann weights

$$T(s|t) = \prod_{j=1}^{m/2} w(s_{2j-1}, s_{2j}, s_{2j+1}, t_{2j-2}, t_{2j-1}, t_{2j}, t_{2j+1}, t_{2j+2}) \tag{A1}$$

where a typical face abcdefgh is shown in figure 10. For the BNNNI model, we define the weight associated with this face as

$$w(\mathrm{a,b,c,d,e,f,g,h}) = \exp[K(\mathrm{ab+bc+af+cf}) + K'(\mathrm{bd+ce+ag+bh})]. \tag{A2}$$

The sparse factorisation of T is achieved by the introduction of $m/2-1$ auxiliary sets of spins:

$$u^p = \{u_1^p, \ldots, u_{m+4}^p\}$$

$$v = \{v_1, \ldots, v_{m+3}\}$$

with $p = 1, \ldots, r$ where $r = m/2-2$.

The transfer matrix elements in (A1) can then be written as

$$T(s|t) = \sum_{\{u^p\},v} A(s|u^1)B(u^1|u^2)\ldots C(u^r|v)D(v|t) \tag{A3}$$

where

$$A(s|u^1) = w(s_1, s_2, s_3, u_{m+4}^1, u_m^1, u_{m+1}^1, u_{m+2}^1, u_{m+3}^1) \times \delta(s_1, u_1^1)\delta(s_3, u_2^1)\ldots\delta(s_m, u_{m-1}^1) \tag{A4}$$

$$B(u^p|u^q) = w(u_2^p, u_3^p, u_4^p, u_{m-1}^q, u_m^q, u_{m+1}^q, u_{m+2}^q, u_{m+3}^q) \times \delta(u_1^p, u_1^q)\delta(u_4^p, u_2^q)\ldots\delta(u_{m+3}^p, u_{m+1}^q)\delta(u_{m+4}^p, u_{m+4}^q) \tag{A5}$$

$$C(u^r|v) = w(u_2^r, u_3^r, u_4^r, v_{m-1}, v_m, v_{m+1}, v_{m+2}, v_{m+3}) \times \delta(u_1^r, v_1)\delta(u_4^r, v_2)\ldots\delta(u_{m+3}^r, v_{m+1})\delta(u_{m+4}^r, v_{m+3}) \tag{A6}$$

$$D(v|t) = w(v_2, v_3, v_1, t_{m-2}, t_{m-1}, t_m, t_1, t_2)\delta(v_4, t_1)\ldots\delta(v_{m+3}, t_m) \tag{A7}$$

in which $q = p+1$.

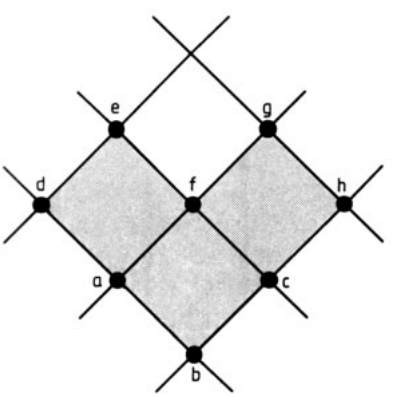

Figure 10. Typical face abcdefgh on the square lattice, drawn diagonally, corresponding to the Boltzmann weight defined in (A2).

The final result from (A3) is

$$\boldsymbol{T} = \boldsymbol{A}\boldsymbol{B}^{m/2-3}\boldsymbol{C}\boldsymbol{D}. \tag{A8}$$

The storage requirements involved in the subsequent computation of the leading eigenvalues of $\boldsymbol{T}$ can be halved by use of spin reversal symmetry.

References

Affleck I 1986 *Phys. Rev. Lett.* **56** 746-8

Barber M N 1983 *Phase Transitions and Critical Phenomena* vol 8, ed C Domb and J L Lebowitz (New York: Academic) pp 145-266

—— 1985 *Physica* **130A** 171-93

Batchelor M T 1986 *J. Aust. Math. Soc.* B in press

Beale P D, Duxbury P M and Yeomans J 1985 *Phys. Rev.* B **31** 7166-70

Blöte H W J, Cardy J L and Nightingale M P 1986 *Phys. Rev. Lett.* **56** 742-5

Cardy J L 1984 *J. Phys. A: Math. Gen.* **17** L385-7

—— 1986 *Phase Transitions and Critical Phenomena* vol 11, ed C Domb and J L Lebowitz (New York: Academic) to appear

Domany E and Kinzel W 1981 *Phys. Rev. Lett.* **47** 5-8

Duxbury P M, Yeomans J and Beale P D 1984 *J. Phys. A: Math. Gen.* **17** L179-84

Faddeev D K and Faddeeva V N 1963 *Computational Methods in Linear Algebra* (San Francisco: Freeman)

Hornreich R M, Liebmann R, Schuster H G and Selke W 1979 *Z. Phys.* B **35** 91-7

Landau D P and Binder K 1985 *Phys. Rev.* B **31** 5946-53

Müller-Hartman E and Zittartz J 1977 *Z. Phys.* B **27** 261-6

Nightingale M P 1976 *Physica* **83A** 561-72

—— 1979 *Proc. K. Neder. Akad. Wet.* **82** 235-91

—— 1982 *J. Appl. Phys.* **53** 7927-32

Oitmaa J and Velgakis M J 1987 *J. Phys. A: Math. Gen.* **20** 1495-505

Selke W 1984 *Modulated Structure Materials* ed T Tsakalakos (Dordrecht: Martinus Nijhoff) pp 23-42

Selke W and Fisher M E 1980 *Z. Phys.* B **40** 71-7

Stephenson J 1970 *J. Math. Phys.* **11** 420-31